

Monitoring Enzymatic Reactions in Real Time Using Venturi Easy Ambient Sonic-Spray Ionization Mass Spectrometry

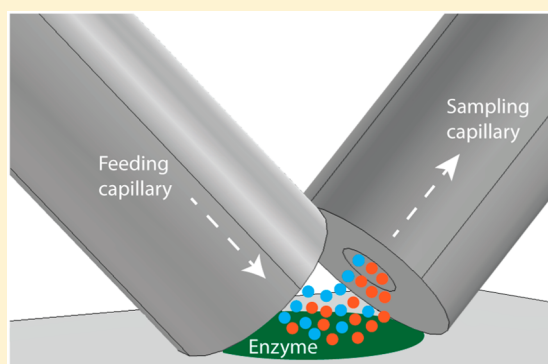
Erik T. Jansson,^{†,‡} Maria T. Dulay,[†] and Richard N. Zare^{*,†}

[†]Department of Chemistry, Stanford University, Stanford, California 94305, United States

[‡]Department of Chemistry–BMC, Uppsala University, SE-75124 Uppsala, Sweden

S Supporting Information

ABSTRACT: We developed a technique to monitor spatially confined surface reactions with mass spectrometry under ambient conditions, without the need for voltage or organic solvents. Fused-silica capillaries immersed in an aqueous solution, positioned in close proximity to each other and the functionalized surface, created a laminar flow junction with a resulting reaction volume of ~ 5 pL. The setup was operated with a syringe pump, delivering reagents to the surface through a fused-silica capillary. The other fused-silica capillary was connected to a Venturi easy ambient sonic-spray ionization source, sampling the resulting analytes at a slightly higher flow rate compared to the feeding capillary. The combined effects of the inflow and outflow maintains a chemical microenvironment, where the rate of advective transport overcomes diffusion. We show proof-of-concept where acetylcholinesterase was immobilized on an organosiloxane polymer through electrostatic interactions. The hydrolysis of acetylcholine by acetylcholinesterase into choline was monitored in real-time for a range of acetylcholine concentrations, fused-silica capillary geometries, and operating flow rates. Higher reaction rates and conversion yields were observed with increasing acetylcholine concentrations, as would be expected.



There has been a recent surge in method development for studies of chemical reactions in real-time with MS. Examples include reactive desorption electrospray ionization (DESI)-MS, where reagents are delivered with an electrospray ionization source to a reactive surface.^{1,2} The droplets bounce off the surface with dried down reagents and are delivered to the MS inlet for detection. Another type of setup involves mixing reagents in a syringe followed by direct infusion to the MS.^{3–7} Hence, the time-course of the reaction can be followed. Similarly, reaction kinetics of colliding droplets sprayed from two different syringes directed at each other have been studied with MS, resulting in reaction rates higher than those obtained in bulk reactions.^{8–10} However, all these techniques rely on electrospray ionization, where several kilovolts of voltage must be applied. Hence, these techniques are incompatible with studies of voltage-sensitive reactions. Also, they do not allow studies of live cells, which rapidly would get electroporated by the high voltage used in electrospray ionization.

We present a new technique, which allows for real-time interrogation of surface reactions with MS without the need for voltage. This was done by coupling a syringe pump connected to a fused-silica capillary outlet with another fused-silica capillary connected to a Venturi easy ambient sonic-spray ionization¹¹ (V-EASI) source. V-EASI does not require voltage to generate charged droplets and relies instead on stochastically generated imbalances of droplet net charge. Further, V-EASI has successfully been used to interrogate several types of

analytes, including small molecules, peptides, proteins, and nucleotides.^{11–14} With our method, the connection of a V-EASI source to the resulting laminar flow junction was used to interrogate chemical reactions taking place on a surface deeply immersed in a liquid. The setup is conceptually similar to a continuous stirred-tank reactor (CSTR).¹⁵ However, because the setup is fully operating in the laminar flow regime and there is no active stirring, mixing with the bulk only takes place through diffusion.

EXPERIMENTAL SECTION

Chemicals. All chemicals were purchased from Sigma-Aldrich (St. Louis, MO). All solvents (MS-grade) were purchased from Thermo Fisher Scientific (Waltham, MA).

Preparation of Organosiloxane Polymer Slides. The organosiloxane polymer was prepared by stirring 500 μL of methyltrimethoxysilane and 225 μL of dimethyldimethoxysilane with 600 μL of 0.12 N acetic acid at room temperature for 30 min. Each of the 12 5 mm round wells on a Teflon-printed glass slide (Electron Microscopy Sciences, Hatfield, PA) was filled with 8 μL of reaction solution. The glass slide was kept in a covered Petri dish during the curing stage of the polymerization in a 65 $^{\circ}\text{C}$ oven for approximately 21 h. The

Received: March 30, 2016

Accepted: June 1, 2016

Published: June 1, 2016

resulting organosiloxane polymers were rinsed free of unreacted starting materials and alcohol byproduct by immersing the slides into a container of acetonitrile and agitating for 45 min. Any acetonitrile remaining on the glass slide and polymers were allowed to evaporate under ambient conditions before deposition of enzyme solution on the surface of the polymer. When not in use, the polymers were stored dry at 4 °C.

Immobilization of Acetylcholinesterase. Acetylcholinesterase was dissolved in 20 mM ammonium bicarbonate buffer, pH 7.8, to a final concentration of 2 μ M. Aliquots of 10 μ L were deposited on the surface of organosiloxane polymers on a glass slide and incubated overnight at room temperature (22–25 °C). The organosiloxane polymers were washed with 20 mM ammonium bicarbonate to remove any unbound acetylcholinesterase. For MS-experiments, the inflowing acetylcholine of various concentrations was also dissolved in 20 mM ammonium bicarbonate.

Real-Time Mass Spectrometry. Fused-silica tubing purchased from Polymicro Technologies (Phoenix, AZ) were used for analyte delivery and sampling. Superfusion was performed with a syringe pump (Harvard Apparatus, Holliston, MA) connected through a PEEK union (IDEX Health & Science, Rohnert Park, CA) to a fused-silica capillary. Sampling was performed with a V-EASI source made from a stainless-steel tee union (Swagelok, Solon, OH). The fused-silica capillary was fitted through the tee union and the attached 10 cm stainless-steel capillary (o.d. 1.59 mm, i.d. 0.51 mm). The fused-silica capillaries were sleeved with fluorinated ethylene propylene tubing sleeves (IDEX Health & Science, Rohnert Park, CA) to fit into the stainless-steel tee, PEEK union (IDEX Health & Science, Rohnert Park, CA) and microelectrode holders (Stoelting, Wood Dale, IL) used for fluidic connections. The microelectrode holders were operated with hydraulic micromanipulators (Narishige, East Meadow, NY), and the capillary tip positions were observed with an inverted microscope (Axiovert 135, Carl Zeiss Microscopy, Thornwood, NY). The microscope was equipped with a motorized *xy*-translational stage (H107, Prior Scientific, Rockland, MA) to facilitate rapid movement of the sample slide.

Mass spectrometry was performed with an LTQ-Orbitrap XL (Thermo Fisher Scientific, Waltham, MA). Mass spectra were acquired across *m/z* 50–500. The capillary temperature was set to 350 °C, capillary voltage was 4 kV, with maximum injection time set to 500 ms per scan for analyte sampling, operating with a N₂ gas pressure at the tee inlet.

Modeling and Data Analysis. Fluid dynamics modeling was performed with COMSOL Multiphysics (COMSOL AB, Stockholm, Sweden). Data acquired with MS was analyzed with MATLAB (Mathworks, Natick, MA). Results are presented as the mean \pm 1 standard deviation.

RESULTS AND DISCUSSION

Liquid-Phase Laminar Flow Junction. The immersed tips of the fused-silica capillaries were operated with micromanipulators under a microscope where the microscopy slide holding the sample for investigation also was placed (Figure 1). Annotated photographs of the setup are shown in Figure S1. By applying a high gas flow in the V-EASI source, directed in parallel with the outlet of the sampling capillary, a local pressure drop caused liquid to be pulled through the capillary and delivered analytes to the inlet of the MS. We performed fluid dynamics modeling of the system, which showed that the slightly higher flow rate used for sampling (0.6 μ L/min)

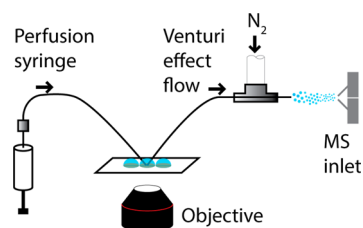


Figure 1. Schematic view of the V-EASI MS setup used for real-time measurements of surface-reactions.

compared to the superfusion flow rate (0.5 μ L/min) was sufficient to have achieved $Pe > 1$ (Péclet number, defined as the ratio of advective transport rate to the diffusive transport rate). As such, a local chemical environment within the bulk solution was maintained with a volume of \sim 5 pL (Figure 2), conceptually similar to superfusion techniques used for electrophysiological cell-studies.^{16,17}

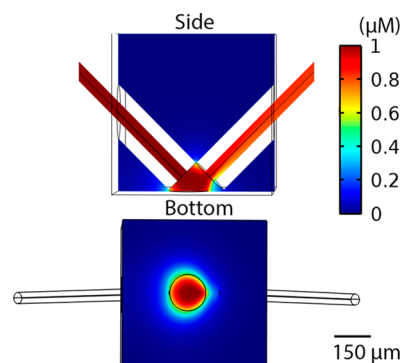
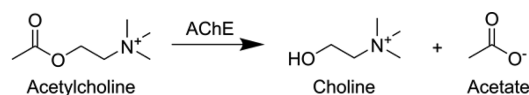


Figure 2. Fluid dynamics modeling of the liquid junction (in the absence of enzymes on the surface) where an analyte was perfused from the left side at 0.5 μ L/min and collected at the right side at 0.6 μ L/min. The scale bar indicates sizes within the colored plane.

Real-Time Monitoring of Hydrolysis of Acetylcholine by Acetylcholinesterase. To provide proof-of-concept of the capabilities of our system, we investigated the reaction kinetics of acetylcholinesterase, an enzyme responsible for termination of acetylcholine signaling in synaptic neurotransmission through rapid hydrolysis of acetylcholine (Scheme 1).¹⁸ Our

Scheme 1. Hydrolysis of Acetylcholine by Acetylcholinesterase (AChE) Yields Choline and Acetate



system monitored the reaction as a function of time and provided information both about transient and steady-state conversions. In our studies, acetylcholinesterase was immobilized on an organosiloxane polymer¹⁹ through electrostatic interactions^{20,21} and was not removed by the relatively low salt concentration (20 mM ammonium bicarbonate) used herein. The flows of the feeding and sampling capillaries were allowed to equilibrate to achieve a steady-state concentration within the liquid junction on the glass microscope slide but outside the area that was functionalized with enzyme. With the fused-silica capillaries locked in position, the automated *xy*-translational stage moved the microscope slide such that the flow junction

went from being in contact with the empty untreated surface to the enzyme surface in ~ 100 ms, traveling at 2 mm/s. To some extent, our system behaved in a similar way as a CSTR, where the apparent reaction rate is initially high and over time approaches zero; the time to reach the steady-state condition depends on the dwell time of molecules within the reaction volume and the kinetics of the reaction itself. Upon arrival at the enzyme surface, acetylcholine was rapidly hydrolyzed into choline and a steady-state was achieved within a few seconds when the feeding concentration was 1 μM acetylcholine (Figure 3). Representative mass spectra for times before and

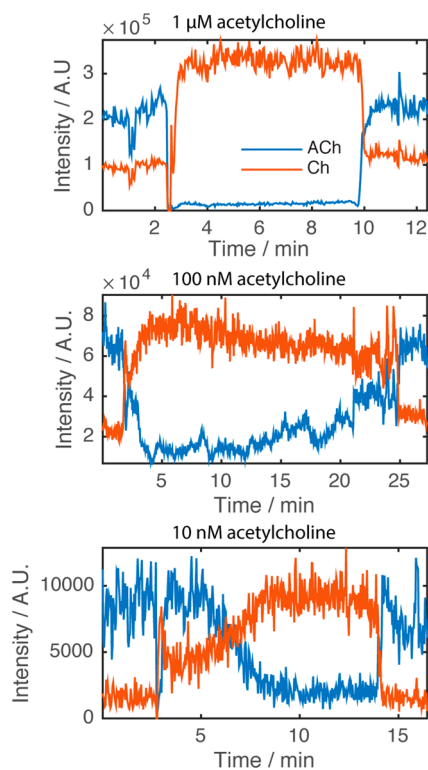


Figure 3. Representative traces of real-time mass spectrometry monitoring conversion of acetylcholine into choline by acetylcholinesterase, surface-bound to an organosiloxane polymer. Use of a small capillary inner diameter (o.d. 150 μm , i.d. 50 μm) and low flow rate ($q_{\text{in}} = 0.5$ $\mu\text{L}/\text{min}$, $q_{\text{out}} = 0.6$ $\mu\text{L}/\text{min}$) allows for a high yield of conversion. The plots show extracted ion chromatograms for acetylcholine (ACh, m/z 146.1176) and choline (Ch, m/z 104.1070). A steady-state condition was first established outside the enzyme surface, followed by a rapid movement (~ 100 ms) into the enzyme surface, which caused a perturbation of the reaction conditions, shortly followed by a new steady-state condition. Moving out from the enzyme surface restored the reaction to its initial conditions.

during exposure of the liquid junction to acetylcholinesterase are shown in Figure S2. Moving the liquid junction out of the enzyme area, levels of acetylcholine and choline returned to their initial levels. By lowering the concentration of acetylcholine, steady-state conditions took progressively longer time to achieve (Figure 3). Data in the range of transient kinetics (normalized to maximum intensity) were fitted with a single exponential of the form $1 - e^{-kt}$ (Figure S3), yielding apparent rate constants k (Table 1). In the steady-state condition, the conversion of acetylcholine into choline X_{ACh} (defined as the difference between inflow and outflow of the acetylcholine

Table 1. Equilibration Rates and Conversion Yields Obtained with Real-Time Mass Spectrometry for Hydrolysis of Acetylcholine with Immobilized Acetylcholinesterase ($n = 3$)

inlet concn (μM)	rate (min^{-1})	conversion (X_{ACh})
1	6.9 ± 2.3	0.936 ± 0.046
0.1	2.4 ± 1.9	0.75 ± 0.26
0.01	0.195 ± 0.048	0.803 ± 0.062

concentration at steady-state divided by the inlet concentration, using the extracted ion current as a measure of relative concentration) was progressively higher with higher substrate concentrations (Table 1).

In conventional CSTRs with active mixing, the conversion yield can be kept constant while scaling up the volume of the system, by keeping the space time parameter τ (reaction volume-to-flow ratio) constant. In contrast, Figures 3 and 4

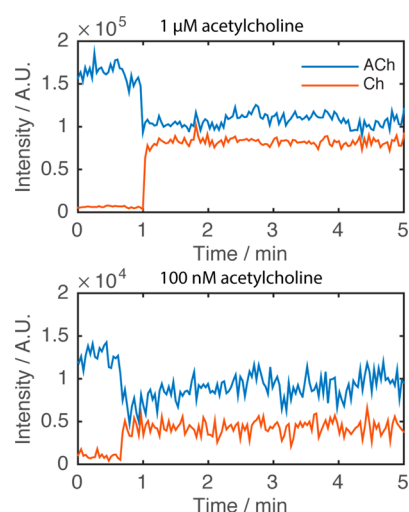


Figure 4. Representative traces of real-time mass spectrometry monitoring conversion of acetylcholine (ACh, m/z 146.1176) into choline (Ch, m/z 104.1070) by acetylcholinesterase. Use of a large capillary inner diameter (o.d. 350 μm , i.d. 200 μm) and higher flow rate ($q_{\text{in}} = 8$ $\mu\text{L}/\text{min}$, $q_{\text{out}} = 10$ $\mu\text{L}/\text{min}$) leads to a low surface-to-volume ratio in combination with less time for substrate diffusion, resulting in lower conversion compared to what is obtained with smaller capillaries and lower flow rates.

show different conversion yields during superfusion with 1 μM acetylcholine at the inlet, where $X_{\text{ACh},50} = 0.936 \pm 0.046$ and $X_{\text{ACh},200} = 0.380 \pm 0.095$ ($p = 0.0008$, Student's t -test, $n = 3$), respectively, while the space time for both systems were similar ($\tau_{50} = 0.2$ s and $\tau_{200} = 0.3$ s), approximating the reaction volume as a half-sphere centered between the capillaries. We hypothesize the reason for this difference is that in contrast to well-mixed CSTRs, the reaction only takes place on a surface and mixing only occurs through diffusion. In Figure 3, the geometry of the liquid-flow junction using o.d. 150 μm , i.d. 50 μm capillaries has a larger base surface-to-volume ratio than in Figure 4, where o.d. 350 μm , i.d. 200 μm capillaries were used. Fluid dynamics modeling confirmed that a higher yield of conversion is to be expected (data not shown) with the experimental setup used in Figure 3 ($q_{\text{in}} = 0.5$ $\mu\text{L}/\text{min}$, $q_{\text{out}} = 0.6$ $\mu\text{L}/\text{min}$) compared to the setup used in Figure 4 ($q_{\text{in}} = 8$ $\mu\text{L}/\text{min}$, $q_{\text{out}} = 10$ $\mu\text{L}/\text{min}$).

Evaluation of Optimal Operating Parameters for Real-Time Mass Spectrometry. The experimental parameters used herein were based on an evaluation of the effects of nitrogen-gas pressure, capillary geometry, and length on signal intensity using a 1 μM acetylcholine solution dissolved in 20 mM ammonium bicarbonate (Table 2). A stainless-steel

Table 2. Effects of Capillary Diameter, Pressure, Capillary Length, and Flow Rate on Signal Intensity and Noise

o.d. (μm)	i.d. (μm)	P (psi)	L (mm)	q ($\mu\text{L}/\text{min}$)	signal (A.U./1000)
150	50	80	340	0.19	15.8 \pm 9.8
150	50	120	340	0.63	214 \pm 14
150	50	160	340	0.76	32.9 \pm 9.4
350	75	80	415	0.62	45.4 \pm 5.0
350	75	120	415	1.25	282 \pm 11
350	75	160	415	2.16	827 \pm 26
350	200	60	835	10	242 \pm 9.7

capillary (o.d. 1.59 mm, i.d. 0.51 mm) was used to hold different sizes of fused-silica capillaries in the V-EASI source. Increasing pressure within the testing range and the resulting increased flow rate monotonically improved the signal intensity for fused-silica capillary with o.d. 350 μm , i.d. 75 μm . However, for the o.d. 150 μm , i.d. 50 μm capillary we found a local maximum for signal intensity at 120 psi nitrogen-gas pressure. The obtained signal intensity (mean and standard deviation obtained from data points collected over a 1 min time-course) was comparable to those resulting from the use of larger capillary sizes but operating at up to 16 times lower flow rate. These results indicated that with a sampling flow rate of 0.6 $\mu\text{L}/\text{min}$, ultimately used in this study, we could minimize sample consumption while maintaining a high signal intensity.

CONCLUSIONS

We have shown proof-of-concept for a novel technique which permits real-time interrogation of liquid-surface reactions with MS without the need of voltage. Several neurotransmitters and neuropeptides are nonoxidizable; hence, they cannot be directly detected with conventional amperometry. We consider that our technique may become complementary to existing techniques for live-cell measurements in future studies.

ASSOCIATED CONTENT

Supporting Information

The Supporting Information is available free of charge on the ACS Publications website at DOI: 10.1021/acs.analchem.6b01246.

Description of the experimental setup, mass spectra, and an example of data fitting (PDF)

AUTHOR INFORMATION

Corresponding Author

*E-mail: rnz@stanford.edu. Phone: (650) 723-3062.

Author Contributions

The manuscript was written through contributions of all authors. All authors have given approval to the final version of the manuscript.

Notes

The authors declare no competing financial interest.

ACKNOWLEDGMENTS

The project was supported by the National Institutes of Health, Award No. R41 GM113337 from the National Institute of General Medical Sciences and Award No. R21 DA039578 from the National Institute on Drug Abuse. E.T.J. was supported by the Swedish Research Council, through Award No. 2015-00406.

REFERENCES

- (1) Huang, G.; Chen, H.; Zhang, X.; Cooks, R. G.; Ouyang, Z. *Anal. Chem.* **2007**, *79*, 8327–8332.
- (2) Perry, R. H.; Splendore, M.; Chien, A.; Davis, N. K.; Zare, R. N. *Angew. Chem., Int. Ed.* **2011**, *50*, 250–254.
- (3) Burkhardt, T.; Letzel, T.; Drewes, J. E.; Grassmann, J. *Biochim. Biophys. Acta, Gen. Subj.* **2015**, *1850*, 2573–2581.
- (4) Lee, E. D.; Mueck, W.; Henion, J. D.; Covey, T. R. *J. Am. Chem. Soc.* **1989**, *111*, 4600–4604.
- (5) Denhart, N.; Letzel, T. *Anal. Bioanal. Chem.* **2006**, *386*, 689–698.
- (6) van den Heuvel, R. H. H.; Gato, S.; Versluis, C.; Gerbaux, P.; Kleanthous, C.; Heck, A. J. R. *Nucleic Acids Res.* **2005**, *33*, e96.
- (7) Yu, Z.; Chen, L. C.; Mandal, M. K.; Nonami, H.; Erra-Balsells, R.; Hiraoka, K. *J. Am. Soc. Mass Spectrom.* **2012**, *23*, 728–735.
- (8) Liu, P.; Zhang, J.; Ferguson, C. N.; Chen, H.; Loo, J. A. *Anal. Chem.* **2013**, *85*, 11966–11972.
- (9) Lee, J. K.; Kim, S.; Nam, H. G.; Zare, R. N. *Proc. Natl. Acad. Sci. U. S. A.* **2015**, *112*, 3898–3903.
- (10) Bain, R. M.; Pulliam, C. J.; Cooks, R. G. *Chem. Sci.* **2015**, *6*, 397–401.
- (11) Santos, V. G.; Regiani, T.; Dias, F. F. G.; Romão, W.; Jara, J. L. P.; Klitzke, C. F.; Coelho, F.; Eberlin, M. N. *Anal. Chem.* **2011**, *83*, 1375–1380.
- (12) Antonakis, M. M.; Tsigotaki, A.; Kanaki, K.; Milios, C. J.; Pergantis, S. A. *J. Am. Soc. Mass Spectrom.* **2013**, *24*, 1250–1259.
- (13) Kanaki, K.; Pergantis, S. A. *Rapid Commun. Mass Spectrom.* **2014**, *28*, 2661–2669.
- (14) Na, N.; Shi, R.; Long, Z.; Lu, X.; Jiang, F.; Ouyang, J. *Talanta* **2014**, *128*, 366–372.
- (15) Schmal, M. *Chemical Reaction Engineering: Essentials, Exercises and Examples*; CRC Press, Taylor & Francis Group: Boca Raton, FL, 2014.
- (16) Veselovsky, N. S.; Engert, F.; Lux, H. D. *Pfluegers Arch.* **1996**, *432*, 351–354.
- (17) Ainla, A.; Jansson, E. T.; Stepanyants, N.; Orwar, O.; Jesorka, A. *Anal. Chem.* **2010**, *82*, 4529–4536.
- (18) Schumacher, M.; Camp, S.; Maulet, Y.; Newton, M.; MacPhee-Quigley, K.; Taylor, S. S.; Friedmann, T.; Taylor, P. *Nature* **1986**, *319*, 407–410.
- (19) Dulay, M. T.; Eberlin, L. S.; Zare, R. N. *Anal. Chem.* **2015**, *87*, 12324–12330.
- (20) Silman, I.; Futerman, A. H. *Eur. J. Biochem.* **1987**, *170*, 11–22.
- (21) Turturk, H.; Yüsekdog, H. *Artif. Cells, Nanomed., Biotechnol.* **2016**, *44*, 443–447.